

Instant Preference Alignment for Text-to-Image Diffusion Models

Yang Li¹, Songlin Yang², Xiaoxuan Han¹, Wei Wang^{1*}, Jing Dong¹, Yueming Lyu³, Ziyu Xue⁴

¹New Laboratory of Pattern Recognition, CASIA, ²The Hong Kong University of Science and Technology

³Nanjing university, ⁴Academy of Broadcasting Science, NRTA

Abstract

Text-to-image (T2I) generation has greatly enhanced creative expression, yet achieving preference-aligned generation in a real-time and training-free manner remains challenging. Previous methods often rely on static, pre-collected preferences or fine-tuning, limiting adaptability to evolving and nuanced user intents. In this paper, we highlight the need for instant preference-aligned T2I generation and propose a training-free framework grounded in multimodal large language model (MLLM) priors. Our framework decouples the task into two components: preference understanding and preference-guided generation. For preference understanding, we leverage MLLMs to automatically extract global preference signals from a reference image and enrich a given prompt using structured instruction design. Our approach supports broader and more fine-grained coverage of user preferences than existing methods. For preference-guided generation, we integrate global keyword-based control and local region-aware cross-attention modulation to steer the diffusion model without additional training, enabling precise alignment across both global attributes and local elements. The entire framework supports multi-round interactive refinement, facilitating real-time and context-aware image generation. Extensive experiments on the Viper dataset and our collected benchmark demonstrate that our method outperforms prior approaches in both quantitative metrics and human evaluations, and opens up new possibilities for dialog-based generation and MLLM-diffusion integration.

1 Introduction

Text-to-image (T2I) generation has significantly boosted user creativity, yet efficiently achieving preference-aligned generation remains a pressing challenge. Previous approaches rely on pre-collected data, assuming user preferences remain unchanged. However, user preferences inherently exhibit strong temporal dynamics and are multifaceted. Therefore, it is essential for T2I models to adapt dynamically to user preferences at inference time. In this paper, we highlight the need for instant preference-aligned generation.

Typically, preference-aligned image generation involves two key components: **Preference Understanding**, capture user preference signals with provided information, and **Preference-Guided Generation**, guide image generation

*Wei Wang is the corresponding author

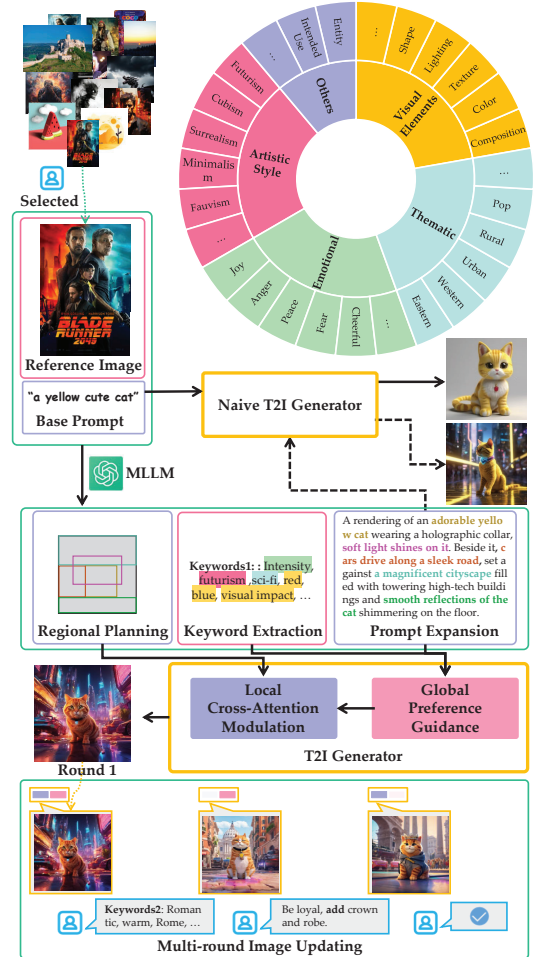


Figure 1: Overview of our instant preference-aligned T2I framework. It decouples the task into preference understanding and preference-guided generation, enabling training-free, real-time, multi-round generation.

with the preference signals. However, instant preference-aligned generation imposes stricter requirements:

(1) In the preference understanding stage, the system must efficiently infer multifaceted and nuanced preferences, even from minimal input (e.g., a single image). Approaches like Viper (Salehi et al. 2024) rely on labor-intensive human ex-

pert acquisition, which introduces a significant delay that hinders its adaptability to rapidly evolving preferences. Alternatively, other techniques (Ruiz et al. 2023; Li et al. 2024; Wang et al. 2024; Salehi et al. 2024; Shen et al. 2024) leverage pretrained models for specific object or style preference extraction, yet they often lack a comprehensive understanding of user preferences and overlook critical contextual content, leading to poor preference alignment.

(2) In the preference-guided generation stage, a major challenge lies in seamlessly integrating inferred preferences with contextual information without further fine-tuning. This complexity stems from preferences inherently influencing both global attributes (e.g., artistic style, emotional tone) and local elements (e.g., specific objects or themes) within an image. While Reinforcement Learning from Human Feedback (RLHF) (Wallace et al. 2024; Fan et al. 2024; Black et al. 2023; Zhang et al. 2024; Xu et al. 2023; Von Rütte et al. 2023) has proven effective in aligning models with general human preferences, it requires additional training and relies on coarse-grained feedback signals, making it difficult to capture the nuanced influence of preferences on both global attributes and local details, even after extensive learning.

To tackle these challenges, we propose a training-free, instant-preference-aligned image generation framework with MLLM priors, encompassing both preference understanding and preference-guided generation.

For the *understanding* stage, unlike Viper (Salehi et al. 2024), which necessitates manual preference definition by expert users, we leverage MLLM to analyze reference images, extracting global keywords that reflect the image’s overall tone, texture, and other salient features. To enhance the comprehensiveness of the keywords, we introduce four critical categories of preference priors: artistic style, emotional/atmospheric resonance, thematic, and visual elements. As shown in Table 3, these four categories cover the vast majority of user preferences. Subsequently, the MLLMs are instructed to perform fine-grained enrichment for a given base prompt, utilizing comprehensive keywords and context content from reference images to generate a detailed preference-aligned prompt.

For *generation* stage, to facilitate seamless integration of preference features without additional training, we introduce the preference guidance at both global and local levels. Specifically, the global preference guidance is adopted to steer image generation using preference keywords, thereby maintaining coherence with the reference images. Furthermore, our local cross-attention modulation applies region constraints to modulate the attention mechanism, ensuring precise control over spatially grounded attributes, facilitating the placement and rendering of preference-relevant elements and visual details.

Crucially, the entire framework supports interactive feedback at each stage, enabling real-time, multi-round refinement, toward more precise and preference-aligned image generation. Extensive experiments demonstrate our method significantly outperforms comparison methods in both metrics and user studies on the Viper Dataset (Salehi et al. 2024) and our collected dataset, achieving superior instant

preference-aligned image generation capability.

Our contributions can be summarized as:

- We pioneer the instant preference alignment framework for real-time T2I generation, advancing dynamic adaptation to multifaceted and evolving preferences.
- We achieve preference understanding by integrating MLLMs with unique instruction design, thereby profoundly achieving broader and more fine-grained preferences than previous methods.
- For preference-guided generation, we eliminate the fine-tuning burden of prior approaches, achieving effective diffusion model control through a more effective global-local disentanglement at inference time.
- Extensive experiments demonstrate that our method outperforms previous approaches and supports multi-round interactive refinement, opening up new possibilities for dialog-based generation and the integration of LLMs with diffusion models.

2 Related Work

2.1 Preference Alignment of T2I Generation

Generative models (Rombach et al. 2022) are typically trained on large-scale datasets, resulting in generally applicable image outputs. There has been growing interest in tailoring T2I models to better align with human preferences. Methods for aligning T2I outputs with user requirements can be broadly divided into two primary categories:

Preference Learning. Methods (Clark et al. 2023; Prabhudesai et al. 2023; Fan et al. 2024; Black et al. 2023) utilize reinforcement learning (Fan et al. 2024; Black et al. 2023) or direct preference optimization (Wallace et al. 2024) to align T2I models with stable human preference by fine-tuning diffusion models using preference data pairs (Xu et al. 2023; Kirstain et al. 2023; Wu et al. 2023). While these methods substantially improve the quality and aesthetics of generated images, they require extensive training data and necessitate large-scale retraining to adapt to new preferences. Other approaches incorporate binary feedback (Von Rütte et al. 2023) or ranking strategies (Tang, Rybin, and Chang 2023) during training, but they often yield suboptimal results due to their limited feedback information.

Customized Content Generation. The customized content generation aims to generate images aligned with user-specified content. Subject customization methods encode user-specified subjects into generated images via fine-tuning models (Gal et al. 2022; Ruiz et al. 2023; Li et al. 2024) or training an encoder (Ye et al. 2023). Meanwhile, style transfer (Wang et al. 2024; Hertz et al. 2024) focuses on learning image style from a reference image and then incorporating it into new artwork creation. Prompt Rewrite (Chen et al. 2024) leverages the Large Language Model to rewrite text prompts with user historical artistic style preferences. Similarly, Viper (Salehi et al. 2024) explores visual preference alignment (i.e., color palette, vibe, and lighting) by collecting style attributes from expert comments, which lacks scalability for diverse preferences at scale. Collectively, existing methods primarily focus on either subjects or styles,



Figure 2: Examples of T2I generations aligned with preferences spanning art styles, visual elements, emotion, and thematic combinations are presented. Each image integrates preference features from reference images with base prompts. The successful incorporation of global attributes, such as color palettes, and additional entities further enhances alignment with the reference images. For instance, the image in the fourth row and second column distinctly showcases a black and gray color scheme alongside broken cars, exemplifying enhanced preference alignment.

neglecting the multifaceted nature of preferences (e.g., emotion, theme-related objects, style, and their mixture) during image generation. To bridge this gap, we propose leveraging MLLMs to automatically understand diverse preference signals from an informative user-preferred image and integrating real-time user feedback, enabling a more comprehensive and adaptable preference-aligned image generation.

2.2 Spatial-Conditioned Image Generation

These methods aim to improve the compositional generation ability of T2I models by using priors from segmentation maps, layouts, sketches, and etc. Getting it Right (Chatterjee et al. 2025) seeks to retrain the diffusion model with a large-scale spatially focused dataset. Other methods (Zhang, Rao, and Agrawala 2023; Li et al. 2023; Avrahami et al. 2023; Wu et al. 2024; Mou et al. 2024) mainly train additional modules into the diffusion model for spatial-condition injection. In contrast, training-free methods manipulate the inference phase by optimizing the cross-attention map (Chen, Laina, and Vedaldi 2024; Chefer et al. 2023) or image latents (Lian et al. 2023; Liu et al. 2022) according to spatial or semantic constraints from labeled data or MLLM output (Lian et al. 2023; Yang et al. 2024). Despite their benefits, these training-free methods currently offer only coarse compositional control, leading to unsatisfactory image generation, especially when dealing with complex prompts.

3 Method

Our preference-guided T2I framework can be summarized as: (1) **Understanding: Preference-Aligned Prompt Enrichment**. Given preferred reference images (or other information), the goal is to enrich a prompt that aligns with the multifaceted preferences. This process involves extracting key preference features from the reference image and enriching the base prompt to reflect the multiple preference

contexts while maintaining the semantic meaning of the base prompt. (2) **Generation: Preference-guided T2I**. Using the preference-aligned prompt, the T2I model generates an image that not only reflects the global attributes but also exhibits the preference-aligned local elements described in the enriched prompt.

3.1 Preliminary

Diffusion-Based T2I Generation. The Stable Diffusion Model (Rombach et al. 2022; Podell et al. 2023), which integrates CLIP Text Model (Radford et al. 2021) $\mathcal{T}_{text}(\cdot)$, VAE (Razavi, Van den Oord, and Vinyals 2019), and a latent U-Net (Ho, Jain, and Abbeel 2020) $\epsilon_{\theta}(\cdot)$, plays a crucial role in text-to-image generation. Given any user-provided prompt y , the latent U-Net denoiser $\epsilon_{\theta}(\cdot)$ is trained as:

$$\mathcal{L} = \mathbb{E}_{\mathbf{x} \sim \mathcal{E}(\mathcal{I}), \epsilon \sim \mathcal{N}(0,1), t} [\|\epsilon - \epsilon_{\theta}(\mathbf{x}_t, t, \mathcal{T}_{text}(y))\|], \quad (1)$$

where t is the timestep, ϵ denotes for the unscaled noise, and \mathbf{x}_t is the noised latent.

Cross-Attention for Text Condition. The latent image feature \mathbf{z} is updated based on the prompt y through cross attention module as follows:

$$\mathbf{Q} = \mathbf{W}^q \mathbf{z}, \mathbf{K} = \mathbf{W}^k \mathcal{T}_{text}(y), \mathbf{V} = \mathbf{W}^v \mathcal{T}_{text}(y), \quad (2)$$

$$\text{Attention}(\mathbf{Q}, \mathbf{K}, \mathbf{V}) = \text{Softmax}\left(\frac{\mathbf{Q}\mathbf{K}^T}{\sqrt{d}}\right)\mathbf{V}. \quad (3)$$

where d is the output dimension of **Key** and **Query**, \mathbf{W}^q , \mathbf{W}^k , and \mathbf{W}^v map the inputs to **Query**, **Key**, and **Value** features, respectively.

3.2 Preference-Aligned Prompt Enrichment

This process can be divided into two steps: Firstly, using the MLLMs to extract the keywords from the preferred reference images. Secondly, enriching the given prompt based on these preference keywords.

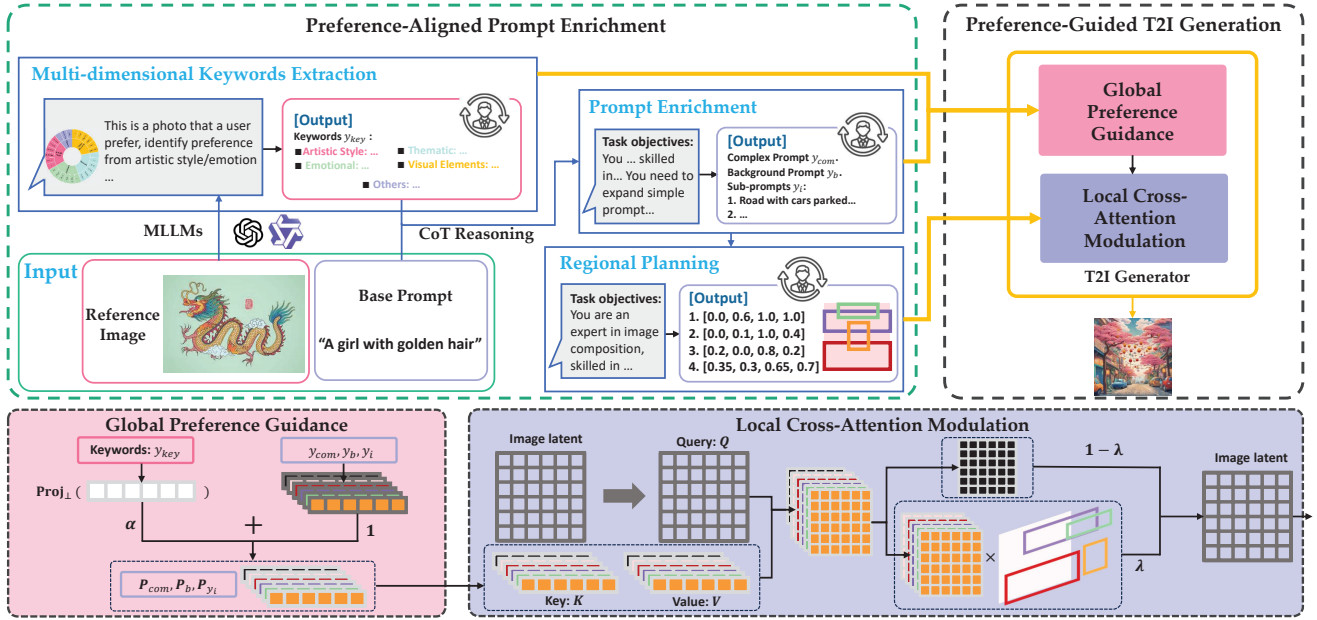


Figure 3: Overview of our preference-guided T2I framework. (1) **Preference-Aligned Prompt Enrichment**, which leverages MLLMs to extract keywords from reference images and enrich the entity description based on these keywords. (2) **Preference-Guided T2I Generation**, which uses global preference guidance for overall alignment, and applies local cross-attention modulation with regional constraints to facilitate fine-grained preference-aligned visual rendering.

Multi-dimensional Keywords Extraction. We systematically classify preference content into Artistic Style, Emotional/Atmospheric Resonance, Thematic, Visual Elements, and other hard-to-classify preferences. This enables the extraction of a richer, tailored signal that integrates both high-level user concepts and detailed attributes for an enhanced user experience. Let X_p be the querying image that a tested user would prefer. We then leverage a pre-trained MLLM’s strong image understanding and multi-modal chain-of-thought reasoning ability (Zhang et al. 2023) to imitate expert perception of querying images and extract preference keywords:

$$y_{key} = \text{MLLM}_{\text{ext}}(X_p). \quad (4)$$

Keyword-Conditioned Prompt Enrichment. For a target base prompt, different preferences would require distinct descriptions. Therefore, we instruct the MLLM to add contextually-interactable entities that embody the desired preferences. This process generates a complex prompt, denoted as y_{com} , comprising a set of n entities, $\{E_i\}_{i=0}^n = \{E_0, E_1, \dots, E_n\}$. Inspired by RPG (Yang et al. 2024), the MLLM simultaneously refines attribute descriptions for each entity, driven by preference keywords, to enhance their preference alignment. This process is formulated as:

$$\{y_i\}_{i=0}^n = \{y_0, y_1, \dots, y_n\} = \text{MLLM}_{\text{exp}}(\{E_i\}_{i=0}^n, y_{key}), \quad (5)$$

$\{y_i\}_{i=0}^n$ are the sub-prompts for each objects. We also generate a background prompt y_b that does not contain any objects to define the background information. Finally, these are merged with the complex prompt y_{com} to form the expanded prompt group: $\{y_{\text{com}}, \{y_i\}_{i=0}^n, y_b\}$.

3.3 Preference-Guided T2I Generation

In this section, we apply the enriched prompt group for T2I generation. To better guide the model with preference signals, we first employ **Global Preference Guidance** to ensure alignment with global attributes. Subsequently, **Regional Planning** and **Local Cross-Attention Modulation** are utilized to constrain the layout and generation of specific entities, ensuring adherence to the desired visual details.

Global Preference Guidance. We encode the extracted preferences keywords, y_{key} , from each preferred image into the text space using the text encoder $\mathcal{T}_{\text{text}}(\cdot)$. As illustrated in Fig. 3, this encoded preference embedding is added to each prompt in $\{y_{\text{com}}, \{y_i\}_{i=0}^n, y_b\}$ to steer generation towards the preferences of each instance:

$$P_{y_i} = \mathcal{T}_{\text{text}}(y_i) + \alpha \cdot \text{Proj}_{\perp}(\mathcal{T}_{\text{text}}(y_{key})), \quad (6)$$

where Proj_{\perp} projects the preference embedding orthogonally to each prompt embedding, with α controlling the strength of the preference modification. Unlike Viper (Salehi et al. 2024), such a projection operation significantly enhances preference alignment while robustly preserving the original prompt’s context. This process gives us the modified embedding group $\{P_{\text{com}}, \{P_{y_i}\}_{i=0}^n, P_b\}$. The comparison between our method and Viper is outlined in Supp. Sec. C. **Regional Planning.** All sub-prompts $\{y_i\}_{i=0}^n$ are then fed into the MLLM to assign layouts. Since directly querying the MLLM for layout information can lead to inaccuracies, we provide manually curated in-context examples to enhance bounding box prediction accuracy. Specifically, for an image of size $H \times W$, such process assigns corresponding bounding boxes $\{B_i\}_{i=0}^n = \{B_0, B_1, \dots, B_n\}$ for each sub-prompt. Each bounding coordinate is normalized to $[0, 1]$,

within the format $\{x_{\text{left}}, y_{\text{top}}, x_{\text{right}}, y_{\text{bottom}}\}$. Regions not covered by sub-region boxes are considered background. To mitigate occlusion from overlapping boxes, particularly for smaller entities, we sort the generated sub-region boxes and their corresponding embedding in descending order of area. **Local Cross-Attention Modulation.** Even with recent advancements like RPG, diffusion models often struggle to accurately interpret complex prompts, particularly when the nuanced visual details of specified entities and their interrelationships must precisely align with user preferences. To address this challenge, we blend multi-entities, $\{E_i\}_{i=0}^n$, into a unified image using a modified cross-attention mechanism, as shown in Fig. 3. Specifically, at each timestep t , within each cross-attention layer, the embeddings from $\{P_{\text{com}}, \{P_{y_i}\}_{i=0}^n, P_b\}$ are passed in parallel to generate corresponding latent image features $z_t^{\text{com}}, \{z_t^i\}_{i=0}^n$, and z_t^b . This process can be formalized as follows:

$$z_t^i = \text{Attention}(\mathbf{W}^q z_t, \mathbf{W}^k P_i, \mathbf{W}^v P_i), \quad (7)$$

where z_t is the input latent image feature. Then, we replace the generated latent image feature of z_t^b with $\{z_t^i\}_{i=0}^n$ according to the sub-region boxes $\{B_i\}_{i=0}^n$, enabling spatial control over each object. The process can be described as:

$$z_t^b = M_{B_i} \cdot z_t^i + (1 - M_{B_i}) \cdot z_t^b, \quad (8)$$

$$z_t^c = z_t^b, \quad (9)$$

where M_{B_i} is a mask indicating regions within bounding box B_i . The replacement operation follows the descending order specified by **Regional Planning**. To ensure seamless and harmonious blending of the background and objects, we employ a weighted sum of the composed latent image feature z_t^c and the complex latent image feature z_t^{com} to output the final latent image feature z_t .

$$z_t = \lambda \cdot z_t^{\text{com}} + (1 - \lambda) \cdot z_t^c. \quad (10)$$

z_t is the updated latent image feature passed to the next module, and λ is a hyper-parameter balancing individual entity contribution and complex prompt.

4 Experiments

4.1 Experimental Setting

Implementation Details. (1) *Target Models:* Our pipeline is extensible, allowing the integration of diverse MLLMs and Diffusion backbones, as demonstrated in the Supp Sec. D. In the main paper, we choose Qwen-VL-72B and Stable Diffusion XL as the backbones. We carefully design the question templates and in-context examples to trigger the CoT planning for the **Keywords Extraction**, **Prompt Enrichment**, and **Regional Planning**. The details of the templates and in-context examples are provided in the Supp Sec. A. For SDXL, we set the classifier guidance $\omega = 5$ and use the DPM-Solver (Lu et al. 2022) with 30 steps for sampling. (2) *Hyper-Parameters:* We set the hyper-parameters λ and α to 0.2 and 0.7, respectively. (3) *Test Data:* We collect image data from four categories: culture, art, emotion, and movie data. The emotional pictures are selected

from the large-scale visual emotion dataset EmoSet (Yang et al. 2023), while the other images are downloaded from the Internet. An illustration of the dataset can be found in the Supp Sec. A. Moreover, we also include the dataset from Viper (Salehi et al. 2024) to further evaluate the generalization of our framework.

Baseline Selection. We aim to generate images that align with the preferences embedded in the user-provided images. To this end, we compare six State-of-the-Art methods: (1) *No Preference (NP)*. The original base prompt is used to generate images without any additional information. (2) *Fabric (Von Rütte et al. 2023)*. This process iteratively updates the image generation. In each iteration, the new image is conditioned on user-selected liked and disliked images from the generated image pool. This process highlights that, in the absence of fine-grained preference signals, the generation process is prone to overfit, leading to suboptimal results. (3) *MGIE (Fu et al. 2023)*. The method utilizes an MLLM to refine the user’s original editing instructions, ensuring that the modified instructions guide the image editing process toward results aligned with the user’s intent. Our comparison demonstrates that simple object attribute editing fails to align with the preference effectively. (4) *Prompt Rewrite (Chen et al. 2024)*. We prompt the SDXL with the complex prompt y_{com} . This complex prompt ensures the integration of multiple preferred attributes with the base prompt and serves to evaluate the effectiveness of **Preference-Guided T2I Generation**. (5) *Viper (Salehi et al. 2024)*. Viper utilizes a collection of expert comments to summarize visual preferences. It modifies prompt embeddings and Classifier-Free Guidance to incorporate preference signals. We integrate MLLM-extracted keywords with their preference injection module to evaluate the effectiveness of our **Preference-Guided T2I Generation** in comparison to theirs. (6) *InstantStyle (Wang et al. 2024)*. It is adopted to show that merely controlling specific aspects of preference (i.e., the color tone or style) is insufficient to represent user preferences comprehensively.

Evaluation Metrics. We evaluate preference using a suite of metrics, including style consistency, emotion accuracy, base prompt alignment, and keyword alignment. Style consistency is assessed using Style Loss (Frenkel et al. 2025). An Emotion Classifier (Yang, Feng, and Huang 2024) is employed to measure the emotion alignment between the generated and the reference images. CLIP Score (Radford et al. 2021) and ImageReward (Gal et al. 2022) are adopted for assessing the text-image alignment, where the text corresponds to the base prompt and the extracted keywords, respectively. Following recipes in prior work (Lee et al. 2024; Yu et al. 2024) that use MLLM-as-a-judge, we use GPT-4o to evaluate *Thematic* and *Visual Elements* alignment. Furthermore, we conducted user studies to validate the preference alignment. Over 20 participants evaluated approximately ~ 200 generated images, answering roughly ~ 80 questions each to assess alignment with reference images.

4.2 Comparison with Baselines

Qualitative Comparison. Fig. 4 presents visual comparisons. Fabric often yields collapsed images because its

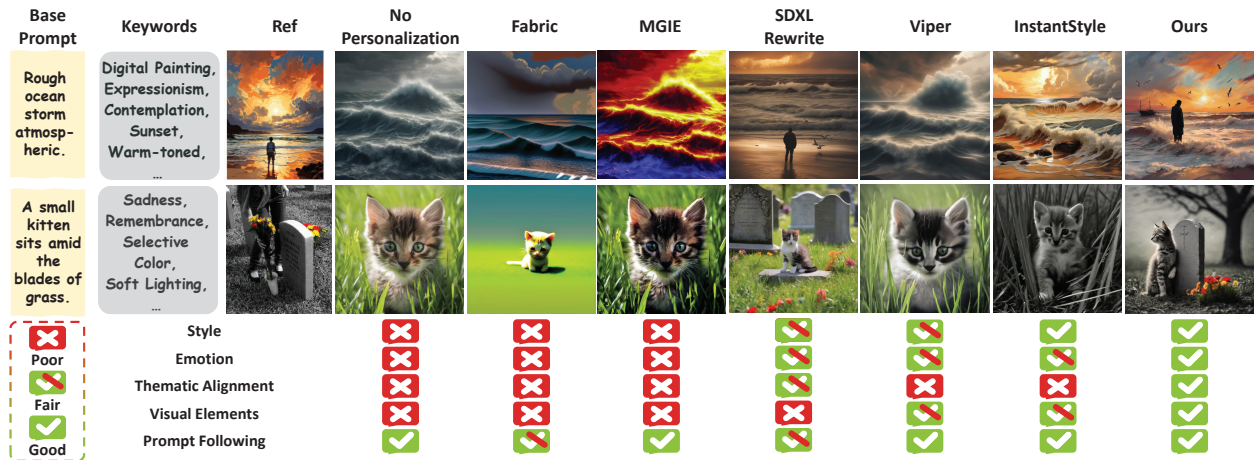


Figure 4: Comparison with baselines. Neither Fabric nor MGIE is capable of generating preference-aligned results. While SDXL Rewrite can produce images close to the reference, it struggles with consistent generation from complex prompts and fails to preserve preference signals. Viper fails to achieve thematic alignment and may lose style and emotion-related elements. InstantStyle solely focuses on transferring reference colors and styles. Finally, our method generates images that adhere to the base prompt while embedding preference signals closely aligned with the reference images.

Table 1: Quantitative comparison with other methods. Our approach achieves optimal overall performance while demonstrating significant advantages in preference studies. The number indicates the percentage of participants who vote for the result. The best results are in highlighted **bold** and the second-best ones are underlined.

Methods	Metrics \uparrow				User Preference Study \uparrow	
	Style Loss	Emo Acc	CLIP Score	ImageReward	Human as Evaluator	GPT-4o as Evaluator
NP	0.569	31.1%	0.295	4.93%	2.21%	2.24%
Fabric	0.556	28.0%	0.245	1.31%	2.04%	2.17%
MGIE	0.593	33.4%	0.283	5.56%	2.93%	3.09%
SDXL Rewrite	0.635	44.2%	0.273	22.3%	9.92%	11.3%
Viper	0.647	42.5%	0.282	<u>23.6%</u>	<u>15.8%</u>	<u>22.4%</u>
InstantStyle	0.712	36.6%	0.252	16.9%	13.9%	14.5%
Ours	<u>0.663</u>	60.2%	<u>0.288</u>	25.4%	53.2%	44.3%

Table 2: Comparing with Viper on the Viper dataset.

	Style Loss	Emo Acc	CLIP Score	ImageReward	Thematic	Visual Elements
Viper	0.69	38.7%	0.276	19.8%	6.01	5.84
Ours	0.77	56.1%	0.278	80.2%	7.12	5.97

Table 3: We design a user study to assess the preference coverage across five categories and the alignment of keywords generated by MLLMs with user preferences.

	Artistic Style	Emotional	Thematic	Visual Elements	Others
PreferenceCoverage (Ratio%)	26.5%	22.9%	21.4%	24.9%	4.3%
Alignment with Users (Accuracy%)	82.3%	85.2%	80.4%	84.7%	—

human feedback is information-sparse and binary. While SDXL Rewrite can roughly reproduce color palettes and themes of the reference image, it struggles to precisely interpret complex prompts and may omit critical visual elements (e.g., the “ship” in the first row). Viper consistently fails to align generated images with preference signals and cannot seamlessly handle local visual details. InstantStyle primarily focuses on image colors or textures, struggles to evoke similar emotions or maintain thematic consistency with reference images. In contrast, our pipeline not only captures

the global preference but also integrates preference-related entities and visual details, generating images that evoke a multifaceted impression similar to reference images while adhering to the base prompt. Please refer to Fig. 2 for additional examples of preference-aligned generation using ours.

Quantitative Comparison. (1) *Preference Understanding:* We conduct a user study to assess the alignment of MLLM-generated preference keywords with user preferences. Participants are presented with a set of images, asked to select their preferred one, and then specify their preference reasons from: artistic style, emotional resonance, thematic, visual elements, and other reasons. This distribution of these selections (Fig. 3, first row) confirms the completeness of our categories. Notably, with only 4.3% of users choosing “Others”. Furthermore, the MLLM-generated keywords achieve over 80.0% alignment accuracy with user preferences, as determined by direct user feedback on keyword relevance to their selections. (2) *Image Generation:* We calculate the Style Loss, Emotion Accuracy, Clip Score, and ImageReward to compare our method with the others. As shown in Table 1, our approach achieves an excellent trade-off between preference alignment and semantic preservation, leading to optimal overall performance. NP, a vanilla text-to-image model, slightly outperforms in CLIP Score

Table 4: Users are presented with pairs of images for preference selection. Then, they are shown groups of images generated from the two different images and asked to pick the one they prefer. The table shows whether the preference signal evoked by generated images still aligns with the preferred images.

	Human as Evaluator	GPT-4o as Evaluator
SDXL Rewrite	68.3%	64.2%
Ours	89.1%	85.7%

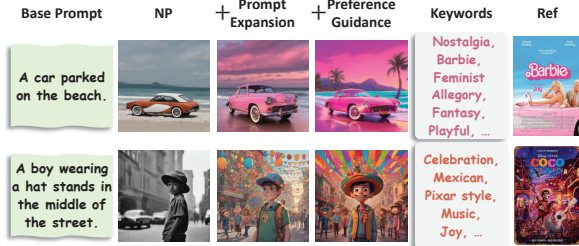


Figure 5: Global Preference Guidance further enhances the alignment of extracted keywords and generated images, e.g., the hat turned to “Mexican Sombrero” in the second row. The preference keywords are listed on the right.

but significantly neglects preference alignment. InstantStyle, designed for style-customized generation and requiring additional training, excels in Style Loss but exhibits a clear performance gap compared to our method in other aspects. SDXL Rewrite and Viper are the closest works to our task, and our method exhibits clear advantages. Moreover, quantitative results on the Viper dataset (Table 2) demonstrate superior performance over Viper and underline the generalization ability of our method.

4.3 User Study

We conduct user studies to evaluate the effectiveness of our pipeline with both human users and GPT-4o (Hurst et al. 2024), performing two types of tests. (1) Users compared images generated by our method against those from other approaches, judging which better captured the essence of the reference image across various dimensions (art style, emotion, theme, visual elements, and others). Our method received nearly twice as much user preference as Viper, as shown in Table 1. (2) Users first selected their preferred image from a pair of distinct images. They were then presented with corresponding generated image groups and asked to choose their preference, assessing whether the preference signals evoked by the generated images aligned with their chosen reference. Our method achieved higher scores in this evaluation, as detailed in Table 4.

4.4 Ablation Study

Global Preference Guidance. We ablate the effect by incrementally incorporating **Prompt Enrichment** and **Global Preference Guidance**. Fig. 5 depicts the results that Global Preference Guidance can further enhance the alignment of extracted keywords and generated images. Further comparison of it with Viper and the ablation of parameter α , please refer to Supp Sec. C.



Figure 6: Ablation study of Local Cross-Attention Modulation. SDXL struggles to generate images aligned with long text, exhibiting attribute obfuscation and entity omission.

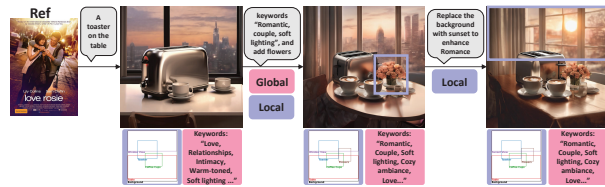


Figure 7: Interaction with real user and MLLMs.

Local Cross-Attention Modulation. When presented with complex prompts, SDXL often struggles to accurately render preference-related visual attributes and their corresponding entities, frequently yielding inadequate content, as shown in Fig. 4. In Fig. 6, our strategy, conversely, facilitates the robust composition of multiple entities by utilizing modified cross-attention, directly addressing this limitation.

4.5 Application: Multi-Round Image Updating

Both quantitative and qualitative evaluations demonstrate the superior performance of our method, even without iterative user feedback. Crucially, our framework inherently further supports multi-round image refinement, a vital capability for real-world instant preference alignment. This includes real-time adjustments to extracted keywords, prompt content, and layout planning. Fig. 7 showcases detailed examples of real-user interactions with our system, illustrating how generated images achieve full alignment with user preferences. Refer to Supp for more results.

5 Conclusion

This paper introduces a training-free framework for instant preference-aligned T2I generation by decoupling preference understanding and guidance. Leveraging MLLM priors, our method enables real-time, fine-grained control over diffusion models without additional tuning. Experiments show superior performance and support for interactive multi-turn refinement, paving the way for preference-aware and dialog-based image generation.

Limitations and Future Work. For preference understanding, due to the limitations of training data of MLLMs, certain minor preferences may not be fully captured (Table 3, “Others”). This can be mitigated by incorporating limited

human feedback (Fig. 7). For generations, current T2I models struggle with certain unseen conditions, as shown in failure cases in Supp. C.

This supplementary material provides additional details as follows.

- A. Implementation Details.
- B. More Comparison.
- C. More Analysis.
- D. Application.

A Implementation Details

A.1 Datasets

We collect image data from four categories: culture, art, emotion, and movie data. Emotional pictures are selected from EmoSet (Yang et al. 2023), while the other images are downloaded from the Internet. We show the images of our dataset in Fig. S8.

A.2 Prompt Templates for MLLMs

We employ MLLMs to mimic human reasoning in achieving **Multi-dimensional Keywords Extraction**, **Keyword-Conditioned Prompt Enrichment**, and **Regional Planning**. We show the templates of these modules in the following:

1. Multi-dimensional Keywords Extraction:

Your role is to accurately identify and summarize the artistic style of images, focusing on the art movements and visual techniques. You are familiar with a wide range of traditional and modern art movements (such as Expressionism, Surrealism, Cubism, etc.) and visual techniques (like oil painting, watercolor, digital painting, sculpture, etc.). Your task is to carefully examine images, identify relevant art movements and visual techniques, and generate a list of keywords that succinctly capture the artistic style. You should rely on both your deep understanding of art history and your ability to analyze the visual elements of the image to provide an informed and precise response as follows: 1.Begin by identifying whether the image aligns with any known art movements (e.g., Expressionism, Cubism, Abstract Expressionism, Surrealism, etc.). Look for visual cues such as emotional expression, color contrast, abstraction, or symbolic elements that may indicate a specific movement. 2.focus on the techniques used to create the image. Check for traditional techniques (like oil painting, fresco, or watercolor) or modern ones (such as digital painting, mixed media, or graffiti). 3.Based on the art movements and visual techniques identified, provide 5 summary keywords. If the image corresponds to one of the listed art movements or techniques (e.g., Expressionism, Oil Painting), include those. If there are no direct matches, use your knowledge to suggest relevant keywords based on the visual characteristics you observed. If you are unable to identify enough matches to reach 5 keywords, provide as many relevant keywords as possible, even if the total is fewer than 5. The output should follow the format of the examples below: Example 1 (Van Gogh's Starry Night): Keywords: Expressionism, Oil Painting, Impasto, Post-Impressionism Example 2 (Digital Concept Art): Keywords: Surrealism, Digital Painting, Neon Sculpture, Cyberpunk Aesthetic.

2. Keyword-Conditioned Prompt Enrichment:

MLLMs in reasoning step by step, enabling them to effectively complete the corresponding task with the assistance of in-context examples, much like how humans approach similar tasks.

A.3 Prompt Templates for GPT-4o as Evaluator

We utilize GPT-4o (Hurst et al. 2024) as a human-like evaluator, instructing it to analyze the preference alignment of the generated images from our method and other approaches. The process leverages the few-shot in-context preference learning capability of MLLMs, as demonstrated in prior work (Lee et al. 2024; Yu et al. 2024). The prompt used for this evaluation is provided below.

Part 1: Preference Analysis of a Reference Image You are an expert in visual aesthetics and human preferences for images. Your task is to analyze the following reference image provided by the user and understand why a person might find it appealing. Please analyze the image based on the following five aspects: 1. Art Style, 2. Emotion, 3. Theme, 4. Visual Elements, 5. Others (Optional). After analyzing these five aspects, summarize why you believe a user might like this image overall. Provide a concise explanation that integrates your analysis from the five aspects above. Here is the reference image: Part 2: Image Preference Matching from a Set of Images Then you will be provided with a set of new images. Your task is to choose ONE image from this set that you believe the user would prefer the most, based on the preference profile you established in Part 1 from the reference image. Analyze each image in the set, considering the same five aspects (Art Style, Emotion, Theme, Visual Elements, and Others) you used in Part 1. Choose only ONE image from the set that you believe is the closest match to the user's preference. Format your response as follows: Chosen Image: Image idx Explanation of Choice: Image 3 is chosen because... Here is the set of new images:

A.4 Definition of each preference category

Artistic Style: focuses on the artistic expression and the visual treatment of the image. It includes traditional and modern artistic movements, as well as specific techniques or styles. e.g., Expressionism, Romanticism, Fauvism, Abstract Expressionism, Oil Painting, Watercolor, Acrylics, Tempera, Fresco, Impasto...

Emotional/Atmospheric: about the mood or feeling that the image should evoke. It can reflect both the emotional tone and the general atmosphere of the image. e.g., Sadness, Joy, Nostalgia, Anger, Fear, Love, Peace, Mystery, Serenity, Tension, Elegance, Melancholy, Romanticism...

Thematic: encompasses the subjects, themes, and cultural references in the image. It could refer to specific cultural representations, visual narratives, or conceptual themes. e.g., time, Transience, Cycles of Nature, Survival, Decay, Transformation, Greek Mythology, Christianity, Hinduism, Buddhism, Ancient Egypt, Judaism, Norse Mythology, Christian Allegory, Astrological Symbols...

Visual elements: this category refers to the structural and formal aspects of the image, focusing on the specific visual features such as composition, lines, colors, and textures. e.g., Symmetry, Asymmetry, Rule of thirds, Warm, Cool, Rough, Smooth, Glossy, Straight lines, Curved lines, Organic lines, High contrast, Low contrast...

B More Comparison

B.1 Consistency with the Prompt Intent

In our experiments, we observe that the generated images tend to align with a specific color palette. To demonstrate that our method ensures coherence between the generated images and the base prompt, we present results in Fig. S9, where prompts with specified color palettes are used. Compared to Style Transfer (Wang et al. 2024), our outcomes not only adhere to the base prompt but also incorporate reference-related entities, better aligning with the reference image (e.g., incorporating theme-related objects and conveying a mood consistent with the reference image).



Figure S9: Ablation study of generating images with a specified color palette. Compared with InstantStyle (Wang et al. 2024) our method can maintain the characteristics of base prompt while achieving preference alignment by incorporating entities.

B.2 Execution Time & Alignment Evaluation

We further compare the execution time and the thematic, visual elements alignment with the other methods. The results are depicted in Tab. S5. Our method achieves superior thematic alignment and competitive visual element consistency compared to the training-based InstantStyle, without incurring the substantial time overhead associated with methods like Viper and Fabric.

Table S5: Execution Time & Alignment Evaluation.

	NP	Fabric	Mgie	Rewrite	InstantStyle	Viper	Ours
Thematic↑	3.67	3.45	4.53	6.03	5.12	5.32	7.43
Visual Elements↑	3.42	3.57	4.12	5.49	6.83	6.05	6.32
Execution Time (s)	~7	>180	~12	~100	~10	>180	~180

Table S6: Comparison on T2I-CompBench.

Method	Spatial↑	Non-Spatial↑
RPG	0.468	0.352
Ours	0.603	0.528

B.3 Comparing Our Global Preference Guidance with Viper

The main comparison results in the main paper demonstrate that Viper (Salehi et al. 2024) struggles to generate images that align with the extracted keywords. This limitation can be attributed to: (1) Missing Preference-Aligned Entities, which our proposed prompt enrichment module and local cross-attention modulation effectively address; and (2) The Trade-off Between Preference Alignment and Prompt Fidelity, where their approach tends to distort the original prompt, particularly when conflicts arise with preference keywords. Formally, the generation process of Viper can be formulated as:

$$\epsilon_{vp}(\mathbf{x}_t t) = \epsilon(\mathbf{x}_t, y_{key}, t) \quad (\text{S11})$$

$$\epsilon_{\theta}(\mathbf{x}, t, y) = (1 - \omega)\epsilon(\mathbf{x}, t) + \omega(\epsilon_{\theta}(\mathbf{x}_t, t, y) + \beta\epsilon_{vp}) \quad (\text{S12})$$

where ϵ is the image generation model and ω is the guidance scale. Viper (Salehi et al. 2024) operates within the latent space and relies on classifier-free guidance. This design fundamentally restricts its generalization, particularly to models like Flux.1-dev, and risks entangling semantic disturbances that significantly alter the original semantics. In contrast, our **Global Preference Guidance**:

$$P_{y_i} = \mathcal{T}_{text}(y_i) + \alpha \cdot \text{Proj}_{\perp}(\mathcal{T}_{text}(y_{key})), \quad (\text{S13})$$

is deployed in the text embedding space. It leverages a projection operation to subtract content related to the current semantic context, thereby ensuring semantic preservation during preference alignment. In Fig. S10, we assess the performance of our **Global Preference Guidance** and Viper (Salehi et al. 2024) in original context preserving. Viper (Salehi et al. 2024) struggles to maintain contextual integrity while adhering to preference signals derived from keywords (e.g., adding a hat to the Japanese boy and turning him into a Mexican boy or generating a girl with an Eastern appearance without golden hair on the right side of the figure). Our **Global Preference Guidance** fully preserves the original context while making essential modifications to align with the preference keywords.

B.4 Comparing Our Local Cross Attention Modulation with RPG

RPG (Yang et al. 2024) employs a coarse Complementary Regional Diffusion for compositional generation and utilizes resizing on the latent image feature to ensure each entity’s appearance. However, this coarse compositional control often leads to unsatisfactory image generation for scenes containing multiple entities with intricate positions and action relationships. Furthermore, the resizing operation itself disrupts the latent space, resulting in poor performance characterized by blurring effects, as evidenced in Tab. S6 and Fig. S11. In Tab. S6, we compare the compositional generation performance between our methods and that of RPG. Our method enhances object arrangement and yields superior compositional generation.

C More Analysis

C.1 Ablation on Global Preference Guidance

Ablation of hyperparameter α . We analyze the effect of α by varying its value as a hyperparameter. The results, shown in Fig. S12, demonstrate that as α increases from 0 to 1.1, the generated images become more aligned with the reference image, deviating from general outputs while preserving the content specified by the base prompt.

Ablation of the preference projection. The project operation ensures that semantic modifications prioritize preference alignment while preserving the context of the original prompt. As shown in Fig. S12, without projection, the generated results become less effective and risk disturbing prompt information.

C.2 Ablation of λ

In Fig. S13, we provide the ablation study of hyperparameter λ . We find that the proper value of λ can benefit the conjunction of each entity, while excessive λ could lead to undesirable results.

C.3 Ablation of Full Pipeline

We conduct an ablation study of our full pipeline to evaluate the effect of each module. The results are presented in Fig S14. With **Global Preference Guidance**, the generated images tend to preserve the base prompt while modifying elements such as color and atmosphere. However, this approach alone struggles to align with thematic-related preferences, such as “ocean” that leads to “deep thinking”. By incorporating “ocean” and other entities circled out in red boxes, we can further enhance the emotional resonance of the images, which is achieved by the **Prompt Enrichment** and **Local Cross-attention Modulation**. Additionally, the recaptioning process provides more descriptive and informative details for the entities, which further improves alignment with preference signals. For example, by having the boy wrapped in a blanket in the first column, we enhance the sense of drifting and makes the feeling of “vulnerability” more prominent.

D Application

D.1 Multi-Round Image Updating

Here, we present additional results of Multi-Round Image Updating, as depicted in Fig. S15. Since preferences suggested by MLLMs may not fully align with personal requirements and personal preferences can vary, our framework allows for iterative adjustments and content updating across multiple rounds to better align with individual user preferences. For instance, in step ②, the overall preference shifts from “intensity, futuristic, sci-fi, ...” to “romantic, warm, Rome, ...”. In step ③, in the third row, adding a fire reintroduces a sense of “intensity” to the image.

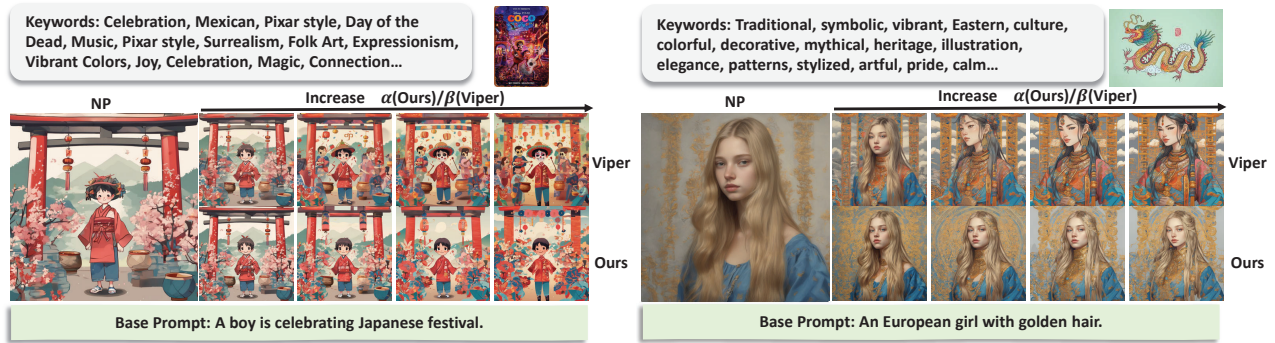


Figure S10: We further give a detailed comparison of our **Global Preference Guidance** with the preference-aligned generation method Viper (Salehi et al. 2024).

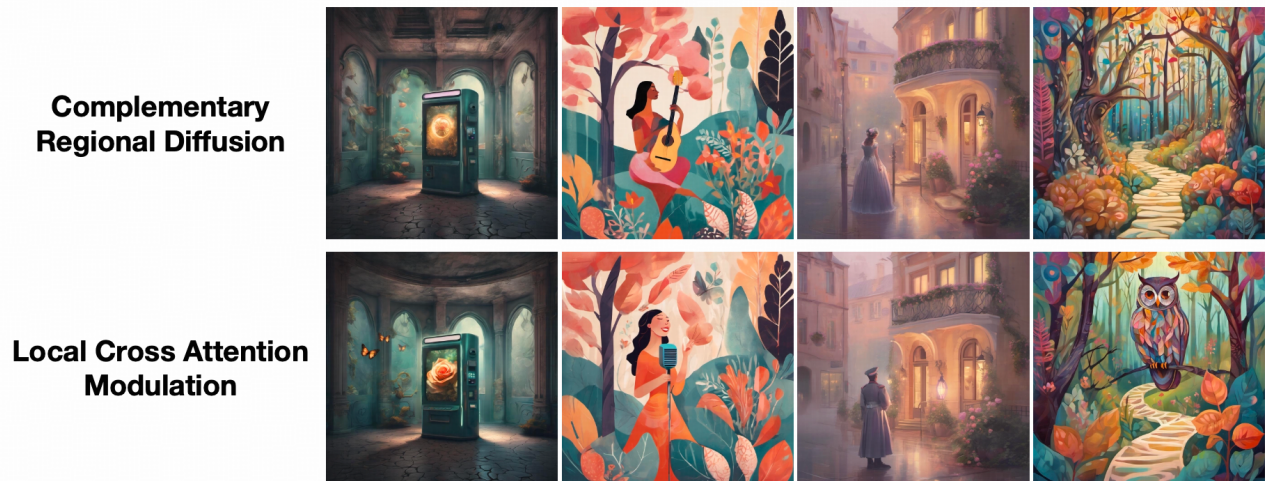


Figure S11: We further give a detailed qualitative comparison of our **Local Cross Attention Modulation** with the **Complementary Regional Diffusion** used in RPG. The RPG method can lead to semantic confusion among entities, resulting in poor alignment where preference-aligned entities are often omitted. The prompts are: (1) “Old vending machine in school hallway”, (2) “A woman singing into a microphone”, (3) “A man in military uniform”, (4) “A barred owl peeking out from tree branches”.

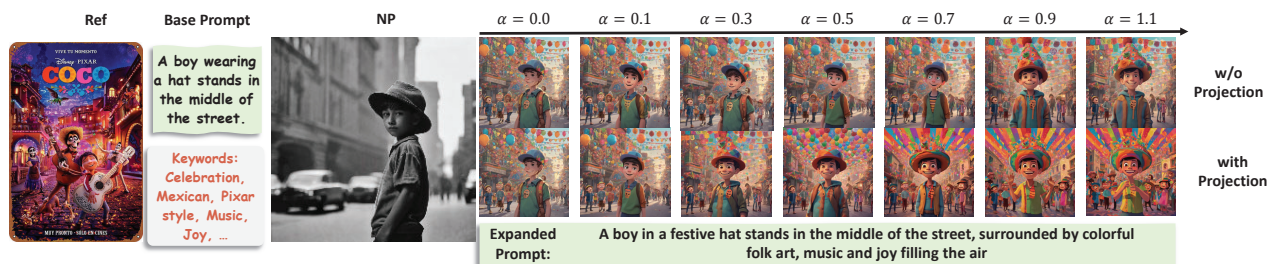


Figure S12: Ablation study of the hyperparameter α and the projection function used in our method.

D.2 Generalizing to Various Backbones

Our framework exhibits a high generalization ability, capable of generalizing to a large range of MLLMs (Fig. S16) and Stable Diffusion backbones (Fig. S17).

(1) **Generalizing to Other MLLMs:** As depicted in Fig. S16, the preference signals extracted by different

MLLMs may vary to some extent, for example, in the case of the first reference image. However, the extracted preferences remain closely aligned with the reference images. Additionally, the flexibility of our framework supports preference adjustments, as demonstrated in the previous **Sec. Multi-Round Image Updating**.

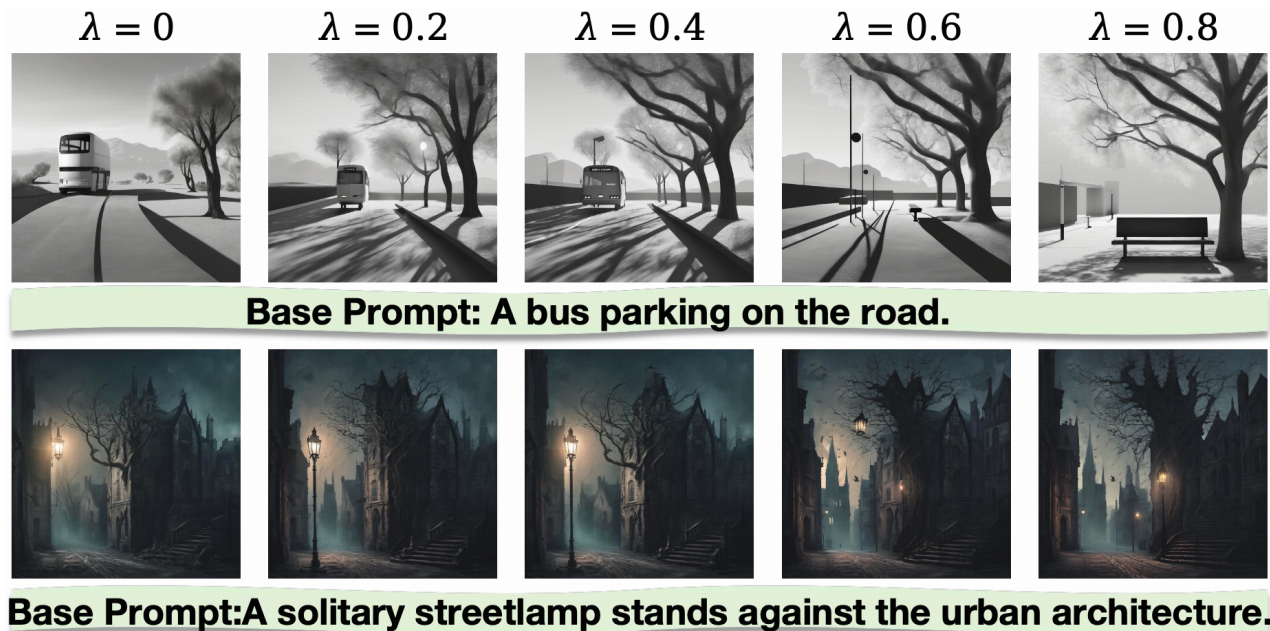


Figure S13: Ablation of the hyperparameter λ in **Local Cross Attention Modulation**.

(2) Generalizing to Other Diffusion Models: As depicted in Fig. S17, the choice of diffusion backbones can influence the generation results; however, the outputs remain consistent with the prompt and preference keywords.

References

- Anthropic. 2024. The Claude 3 Model Family: Opus, Sonnet, Haiku.
- Avrahami, O.; Hayes, T.; Gafni, O.; Gupta, S.; Taigman, Y.; Parikh, D.; Lischinski, D.; Fried, O.; and Yin, X. 2023. Spatext: Spatio-textual representation for controllable image generation. In *Proceedings of the IEEE/CVF Conference on Computer Vision and Pattern Recognition*, 18370–18380.
- Bai, S.; Chen, K.; Liu, X.; Wang, J.; Ge, W.; Song, S.; Dang, K.; Wang, P.; Wang, S.; Tang, J.; et al. 2025. Qwen2. 5-VL Technical Report. *arXiv preprint arXiv:2502.13923*.
- Black, K.; Janner, M.; Du, Y.; Kostrikov, I.; and Levine, S. 2023. Training diffusion models with reinforcement learning. *arXiv preprint arXiv:2305.13301*.
- Chatterjee, A.; Stan, G. B. M.; Aflalo, E.; Paul, S.; Ghosh, D.; Gokhale, T.; Schmidt, L.; Hajishirzi, H.; Lal, V.; Baral, C.; et al. 2025. Getting it right: Improving spatial consistency in text-to-image models. In *European Conference on Computer Vision*, 204–222. Springer.
- Chefer, H.; Alaluf, Y.; Vinker, Y.; Wolf, L.; and Cohen-Or, D. 2023. Attend-and-excite: Attention-based semantic guidance for text-to-image diffusion models. *ACM Transactions on Graphics (TOG)*, 42(4): 1–10.
- Chen, M.; Laina, I.; and Vedaldi, A. 2024. Training-free layout control with cross-attention guidance. In *Proceedings of the IEEE/CVF Winter Conference on Applications of Computer Vision*, 5343–5353.
- Chen, Z.; Zhang, L.; Weng, F.; Pan, L.; and Lan, Z. 2024. Tailored visions: Enhancing text-to-image generation with personalized prompt rewriting. In *Proceedings of the IEEE/CVF Conference on Computer Vision and Pattern Recognition*, 7727–7736.
- Clark, K.; Vicol, P.; Swersky, K.; and Fleet, D. J. 2023. Directly Fine-Tuning Diffusion Models on Differentiable Rewards. *arXiv:2309.17400*.
- Esser, P.; Kulal, S.; Blattmann, A.; Entezari, R.; Müller, J.; Saini, H.; Levi, Y.; Lorenz, D.; Sauer, A.; Boesel, F.; et al. 2024. Scaling rectified flow transformers for high-resolution image synthesis. In *Forty-first International Conference on Machine Learning*.
- Fan, Y.; Watkins, O.; Du, Y.; Liu, H.; Ryu, M.; Boutilier, C.; Abbeel, P.; Ghavamzadeh, M.; Lee, K.; and Lee, K. 2024. Reinforcement learning for fine-tuning text-to-image diffusion models. *Advances in Neural Information Processing Systems*, 36.
- Frenkel, Y.; Vinker, Y.; Shamir, A.; and Cohen-Or, D. 2025. Implicit style-content separation using b-lora. In *European Conference on Computer Vision*, 181–198. Springer.
- Fu, T.-J.; Hu, W.; Du, X.; Wang, W. Y.; Yang, Y.; and Gan, Z. 2023. Guiding instruction-based image editing via multimodal large language models. *arXiv preprint arXiv:2309.17102*.
- Gal, R.; Alaluf, Y.; Atzmon, Y.; Patashnik, O.; Bermano, A. H.; Chechik, G.; and Cohen-Or, D. 2022. An image is worth one word: Personalizing text-to-image generation using textual inversion. *arXiv preprint arXiv:2208.01618*.
- Hertz, A.; Voynov, A.; Fruchter, S.; and Cohen-Or, D. 2024. Style aligned image generation via shared attention. In *Pro-*

ceedings of the IEEE/CVF Conference on Computer Vision and Pattern Recognition, 4775–4785.

Ho, J.; Jain, A.; and Abbeel, P. 2020. Denoising diffusion probabilistic models. *Advances in neural information processing systems*, 33: 6840–6851.

Hurst, A.; Lerer, A.; Goucher, A. P.; Perelman, A.; Ramesh, A.; Clark, A.; Ostrow, A.; Welihinda, A.; Hayes, A.; Radford, A.; et al. 2024. Gpt-4o system card. *arXiv preprint arXiv:2410.21276*.

Kirstain, Y.; Polyak, A.; Singer, U.; Matiana, S.; Penna, J.; and Levy, O. 2023. Pick-a-Pic: An Open Dataset of User Preferences for Text-to-Image Generation. *arXiv:2305.01569*.

Labs, B. F. 2024. FLUX: Inference Repository. <https://github.com/black-forest-labs/flux>. Accessed: 2024-10-25.

Lee, S.; Kim, S.; Park, S.; Kim, G.; and Seo, M. 2024. Prometheus-vision: Vision-language model as a judge for fine-grained evaluation. In *Findings of the Association for Computational Linguistics ACL 2024*, 11286–11315.

Li, Y.; Liu, H.; Wu, Q.; Mu, F.; Yang, J.; Gao, J.; Li, C.; and Lee, Y. J. 2023. Gligen: Open-set grounded text-to-image generation. In *Proceedings of the IEEE/CVF Conference on Computer Vision and Pattern Recognition*, 22511–22521.

Li, Y.; Yang, S.; Wang, W.; and Dong, J. 2024. Beyond inserting: Learning identity embedding for semantic-fidelity personalized diffusion generation. *arXiv preprint arXiv:2402.00631*.

Lian, L.; Li, B.; Yala, A.; and Darrell, T. 2023. Llm-grounded diffusion: Enhancing prompt understanding of text-to-image diffusion models with large language models. *arXiv preprint arXiv:2305.13655*.

Liu, N.; Li, S.; Du, Y.; Torralba, A.; and Tenenbaum, J. B. 2022. Compositional visual generation with composable diffusion models. In *European Conference on Computer Vision*, 423–439. Springer.

Lu, C.; Zhou, Y.; Bao, F.; Chen, J.; Li, C.; and Zhu, J. 2022. Dpm-solver: A fast ode solver for diffusion probabilistic model sampling in around 10 steps. *Advances in Neural Information Processing Systems*, 35: 5775–5787.

Mou, C.; Wang, X.; Xie, L.; Wu, Y.; Zhang, J.; Qi, Z.; and Shan, Y. 2024. T2i-adapter: Learning adapters to dig out more controllable ability for text-to-image diffusion models. In *Proceedings of the AAAI Conference on Artificial Intelligence*, volume 38, 4296–4304.

Pernias, P.; Rampas, D.; Richter, M. L.; Pal, C. J.; and Aubreville, M. 2023. Würstchen: An efficient architecture for large-scale text-to-image diffusion models. *arXiv preprint arXiv:2306.00637*.

Podell, D.; English, Z.; Lacey, K.; Blattmann, A.; Dockhorn, T.; Müller, J.; Penna, J.; and Rombach, R. 2023. Sdxl: Improving latent diffusion models for high-resolution image synthesis. *arXiv preprint arXiv:2307.01952*.

Prabhudesai, M.; Goyal, A.; Pathak, D.; and Fragkiadaki, K. 2023. Aligning Text-to-Image Diffusion Models with Reward Backpropagation. *arXiv:2310.03739*.

Radford, A.; Kim, J. W.; Hallacy, C.; Ramesh, A.; Goh, G.; Agarwal, S.; Sastry, G.; Askell, A.; Mishkin, P.; Clark, J.; et al. 2021. Learning transferable visual models from natural language supervision. In *International conference on machine learning*, 8748–8763. PMLR.

Razavi, A.; Van den Oord, A.; and Vinyals, O. 2019. Generating diverse high-fidelity images with vq-vae-2. *Advances in neural information processing systems*, 32.

Rombach, R.; Blattmann, A.; Lorenz, D.; Esser, P.; and Ommer, B. 2022. High-resolution image synthesis with latent diffusion models. In *Proceedings of the IEEE/CVF conference on computer vision and pattern recognition*, 10684–10695.

Ruiz, N.; Li, Y.; Jampani, V.; Pritch, Y.; Rubinstein, M.; and Aberman, K. 2023. Dreambooth: Fine tuning text-to-image diffusion models for subject-driven generation. In *Proceedings of the IEEE/CVF conference on computer vision and pattern recognition*, 22500–22510.

Salehi, S.; Shafiei, M.; Yeo, T.; Bachmann, R.; and Zamir, A. 2024. ViPer: Visual Personalization of Generative Models via Individual Preference Learning. *arXiv preprint arXiv:2407.17365*.

Shen, X.; Zhang, R.; Zhao, X.; Zhu, J.; and Xiao, X. 2024. Pmg: Personalized multimodal generation with large language models. In *Proceedings of the ACM Web Conference 2024*, 3833–3843.

Tang, Z.; Rybin, D.; and Chang, T.-H. 2023. Zeroth-order optimization meets human feedback: Provable learning via ranking oracles. *arXiv preprint arXiv:2303.03751*.

Team, G.; Anil, R.; Borgeaud, S.; Alayrac, J.-B.; Yu, J.; Soricut, R.; Schalkwyk, J.; Dai, A. M.; Hauth, A.; Millican, K.; et al. 2023. Gemini: a family of highly capable multimodal models. *arXiv preprint arXiv:2312.11805*.

Von Rütte, D.; Fedele, E.; Thomm, J.; and Wolf, L. 2023. Fabric: Personalizing diffusion models with iterative feedback. *arXiv preprint arXiv:2307.10159*.

Wallace, B.; Dang, M.; Rafailov, R.; Zhou, L.; Lou, A.; Pushwalkam, S.; Ermon, S.; Xiong, C.; Joty, S.; and Naik, N. 2024. Diffusion model alignment using direct preference optimization. In *Proceedings of the IEEE/CVF Conference on Computer Vision and Pattern Recognition*, 8228–8238.

Wang, H.; Spinelli, M.; Wang, Q.; Bai, X.; Qin, Z.; and Chen, A. 2024. Instantstyle: Free lunch towards style-preserving in text-to-image generation. *arXiv preprint arXiv:2404.02733*.

Wu, X.; Sun, K.; Zhu, F.; Zhao, R.; and Li, H. 2023. Human Preference Score: Better Aligning Text-to-Image Models with Human Preference. *arXiv:2303.14420*.

Wu, Y.; Zhou, X.; Ma, B.; Su, X.; Ma, K.; and Wang, X. 2024. Ifadapter: Instance feature control for grounded text-to-image generation. *arXiv preprint arXiv:2409.08240*.

Xu, J.; Liu, X.; Wu, Y.; Tong, Y.; Li, Q.; Ding, M.; Tang, J.; and Dong, Y. 2023. ImageReward: Learning and Evaluating Human Preferences for Text-to-Image Generation. *arXiv:2304.05977*.

- Yang, J.; Feng, J.; and Huang, H. 2024. EmoGen: Emotional Image Content Generation with Text-to-Image Diffusion Models. In *Proceedings of the IEEE/CVF Conference on Computer Vision and Pattern Recognition*, 6358–6368.
- Yang, J.; Huang, Q.; Ding, T.; Lischinski, D.; Cohen-Or, D.; and Huang, H. 2023. Emoset: A large-scale visual emotion dataset with rich attributes. In *Proceedings of the IEEE/CVF International Conference on Computer Vision*, 20383–20394.
- Yang, L.; Yu, Z.; Meng, C.; Xu, M.; Ermon, S.; and Bin, C. 2024. Mastering text-to-image diffusion: Recaptioning, planning, and generating with multimodal llms. In *Forty-first International Conference on Machine Learning*.
- Ye, H.; Zhang, J.; Liu, S.; Han, X.; and Yang, W. 2023. Ip-adapter: Text compatible image prompt adapter for text-to-image diffusion models. *arXiv preprint arXiv:2308.06721*.
- Yu, C.; Lu, H.; Gao, J.; Tan, Q.; Yang, X.; Wang, Y.; Wu, Y.; and Vinitzky, E. 2024. Few-shot in-context preference learning using large language models. *arXiv preprint arXiv:2410.17233*.
- Zhang, L.; Rao, A.; and Agrawala, M. 2023. Adding conditional control to text-to-image diffusion models. In *Proceedings of the IEEE/CVF International Conference on Computer Vision*, 3836–3847.
- Zhang, S.; Wang, B.; Wu, J.; Li, Y.; Gao, T.; Zhang, D.; and Wang, Z. 2024. Learning Multi-dimensional Human Preference for Text-to-Image Generation. In *Proceedings of the IEEE/CVF Conference on Computer Vision and Pattern Recognition*, 8018–8027.
- Zhang, Z.; Zhang, A.; Li, M.; Zhao, H.; Karypis, G.; and Smola, A. 2023. Multimodal chain-of-thought reasoning in language models. *arXiv preprint arXiv:2302.00923*.

Keywords

melancholy,
introspection,
vulnerability,
emotional
depth,
ocean, ...

Ref



①

① NP ② Global Guidance ③ Entity ④ Entity Recaption

A child and a penguin sit by the sea.



A little girl stands in the rain.



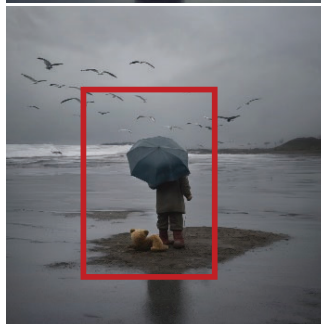
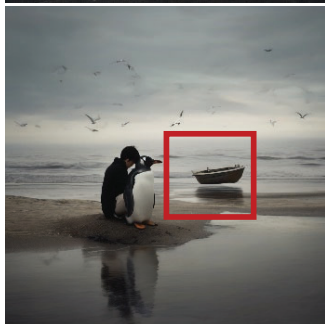
An old man and his dog sit on a couch.



① + ②



① + ② + ③



① + ② + ③ + ④

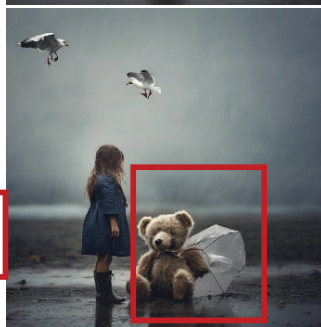


Figure S14: Ablation study of our full pipeline. Global Preference Guidance guides the generated images with preference-aligned elements such as color and atmosphere while preserving the base prompt. By incorporating entities (circled out by the red rectangles), we can further enhance the emotional resonance of the images. Additionally, the recaptioning process provides more descriptive and informative details for the entities, which further improves alignment with preference signals. For example, as we make the boy wearing a blanket in the first column, it enhances a sense of drifting and makes the "vulnerability" more prominent.

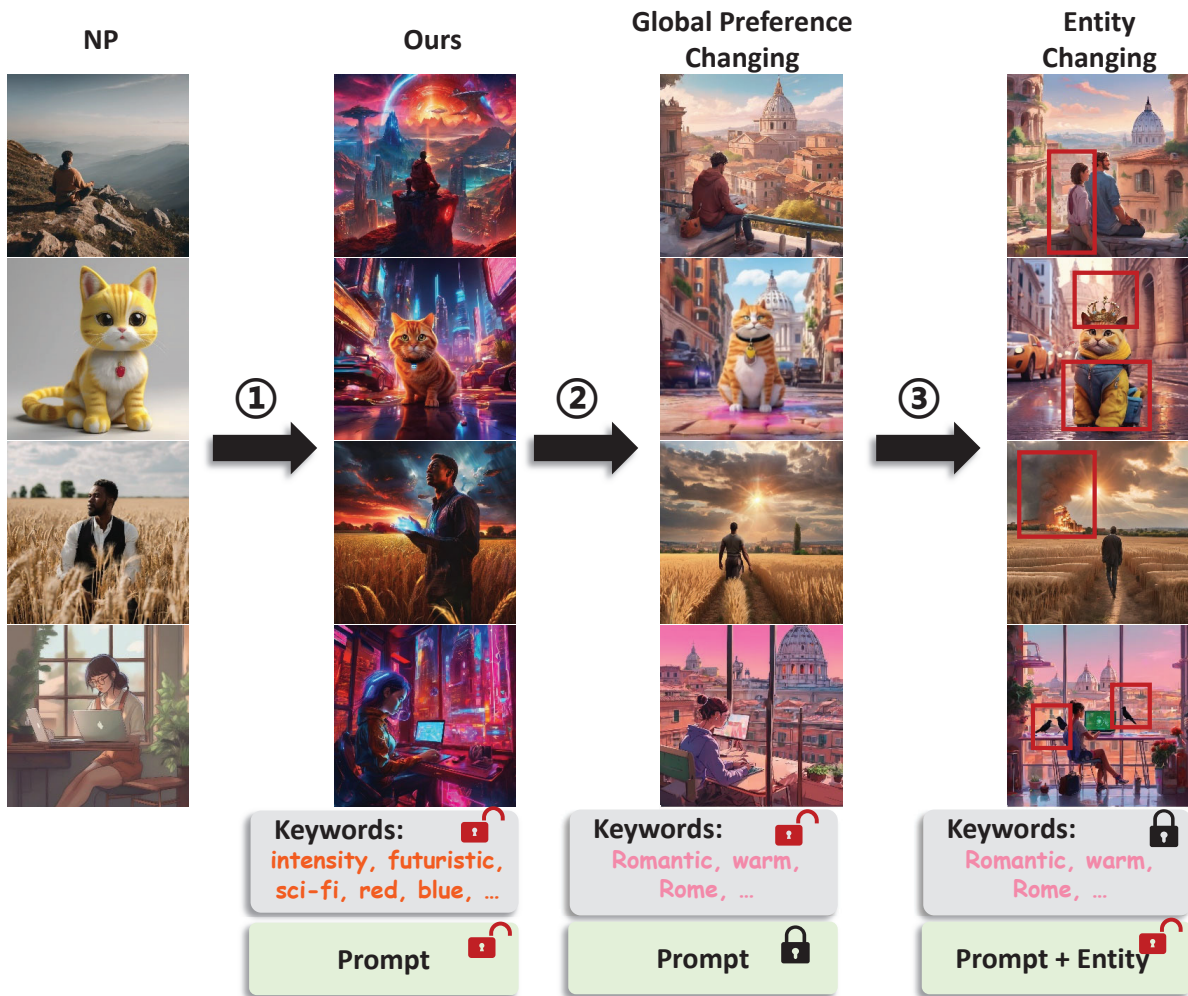


Figure S15: Multi-Round Image Updating. Our framework supports adjusting preferences or updating content to better align with individual user preferences. For entity changes, the modified entities are highlighted with red rectangles.



Figure S16: Generalizing our framework to different MLLMs, including Claude (Anthropic 2024), Gemini (Team et al. 2023), Qwen (Bai et al. 2025), and GPT-4o (Hurst et al. 2024).



Figure S17: Generalizing our framework to different Diffusion backbones, including SD-2.1 (Rombach et al. 2022), Stable-Cascade (Pernias et al. 2023), and SD3-Large (Esser et al. 2024), and Flux.1-dev (Labs 2024).